Morphology and Phase Segregation of Spin-Casted Films of Polyfluorene/PCBM Blends

Svante Nilsson,[†] Andrzej Bernasik,[‡] Andrzej Budkowski,[§] and Ellen Moons*,[†]

Department of Physics, Karlstad University, SE-651 88 Karlstad, Sweden; Faculty of Physics and Applied Computer Science, AGH-University of Science and Technology, Al. Mickiewicza 30, 30-059 Krakow, Poland; and Institute of Physics, Jagiellonian University, Reymonta 4, 30-059 Kraków, Poland

Received March 23, 2007; Revised Manuscript Received August 30, 2007

ABSTRACT: In this study the morphology of spin-casted films of polymers blended with [6,6]-phenyl C_{61}-butyric acid methyl ester (PCBM) has been studied. It was found that the lateral structure formation in the films is favored by rapid solvent evaporation and strong polymer−PCBM repulsion. The formation of homogeneous films is favored by slow evaporation and weak polymer−PCBM repulsion. The effect of solvent evaporation rate is the opposite of what is found for spin-casting polymer−polymer blends. The results can be explained by the kinetics of phase separation and the phase behavior involving limited solubility and crystallization of PCBM.

Introduction

Organic solar cells and light-emitting diodes made from thin films of conjugated polymers are an active area of research.[1−5] In photovoltaic devices a polymer with electron-donating properties is blended with an electron acceptor. Polyfluorene copolymers blended with the C_{60}-derivative PCBM as electron acceptor have shown high potential in solar cell applications. Absorption spectra and electronic structure of the components are obviously important for the operation of the device, but the role of morphology of the blend cannot be ignored, since the charge separation takes place at the donor−acceptor interface and a large interfacial area is obtained by small domain sizes. At the same time it is also important to have continuous paths through both the donor and acceptor phases for efficient charge transport between the electrodes. A polymer−polymer blend in solution is a one-phase system only at low enough solute concentrations. When the solvent evaporates during spin-coating, the increase in concentration will drive the system into a two-phase area with each phase enriched in its respective component. Since the solvent is removed rapidly during the spin-coating (quenching), there is not enough time for equilibrium structures to develop. Many different structures have been reported in the literature for different blend systems with both lateral and vertical segregation on the nano- to micrometer scale. Because of the rapid evaporation of solvent the phase, separation is a complex process often resulting in nonequilibrium morphologies. The morphology also depends on solubility and surface energies of components and substrate. Structure formation models suggest initial formation of multilayers, which can either be frozen in or break up by interfacial instabilities to yield lateral domains.[6−13] Lamellar structures resulting from solvent quench in polymer blend films have been observed. Vertical phase separation by spinodal decomposition has been reported in polymer−polymer blends[12,13,49] and blends containing polyfluorene copolymers.[14−19] Surface segregation can be promoted by substrate surface energy modification[8,10,20,21] and solvent evaporation control.[8,19,21] In a recent study we have shown that surface-directed spinodal decomposition occurs also in a blend of a conjugated polyfluorene copolymer, APFO-3, with the fullerene derivative PCBM, when spin-coated from chloroform.[25] We have also found a weak dependence of this vertical structure on the substrate due to specific interactions of one of the components with the substrate.[53] However, it was found that spin-casted polyfluorene copolymer/PCBM blends form different film structures depending on which polymer and solvent was used.[40,43] In the present study the resulting morphology of spin-coated polyfluorene copolymers/PCBM blends has been studied as a function of surface energy of the pure components and the kinetics of evaporation, with the aim of improving the understanding of the driving forces responsible for film structure formation in these systems.

Experimental Section

Materials. *Chemicals.* Four different polymers have been used. Poly(9,9-dioctylfluorenyl-2,7-diyl) (F8), poly[(9,9-dioctylfluorenyl-2,7-diyl)-*alt*-*co*-(*N*,*N*′-diphenyl-*N*,*N*′di(*p*-butylphenyl)-1,4-diaminobenzene)] (PFB), and poly[(9,9-dioctylfluorenyl-2,7-diyl)-*co*-(1,4-benzo-{2,1′,3}-thiadiazole)] (F8BT) were supplied by American Dye Source Inc., Canada.

Poly[(9,9-dioctylfluorenyl-2,7-diyl)-*co*-5,5-(4′,7′-di-2-thienyl-2′,1′,3′-benzothiadiazole] (APFO-3) was supplied by and synthesized in the group of Prof. M. R. Andersson, Department of Materials and Surface Chemistry/Polymer Technology, Chalmers University of Technology, Sweden. The molecular weights (M_w) were 140 000 for F8, 10 000 for PFB, 30 000 for F8BT, and 11 800 for APFO-3. [6,6]-Phenyl C_{61}-butyric acid methyl ester (PCBM) was purchased from and synthesized in the group of J. C. Hummelen, University of Groningen, The Netherlands. The chemical structures of polymers and PCBM are shown in Figure 1. Chloroform (p.a., Merck), toluene (p.a., Merck), xylene (p.a., Merck), chlorobenzene (p.a., Merck), 2-chlorotoluene (zur synthese, BDH), and mesitylene (zur synthese, Merck) have been used as solvents.

Films were prepared by spin-coating blends of polymer and PCBM dissolved in a solvent. The total solute concentration (polymer + PCBM) was kept constant at 12 mg/mL unless otherwise indicated. A few samples were also prepared using 30 mg/mL. The polymer/PCBM blend ratios used were 1:1, 1:2, 1:3, and 1:4 by weight.

Substrates. Glass, cut from microscope slides, was used as substrate in most cases and cleaned with ethanol. Silicon wafers

* To whom correspondence should be addressed.
† Karlstad University.
‡ AGH-University of Science and Technology.
§ Jagiellonian University.

10.1021/ma070712a CCC: $37.00
Published on Web 10/10/2007

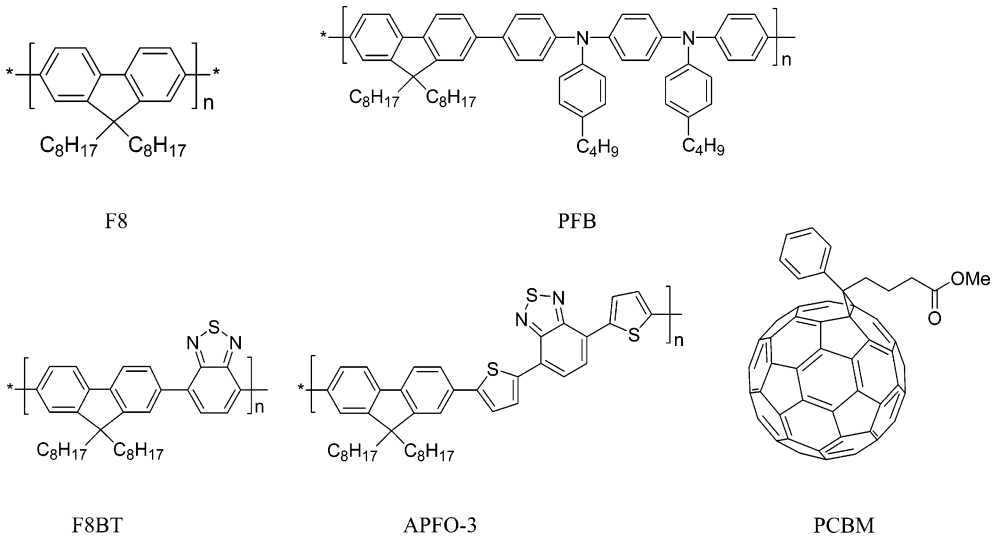

Figure 1. Chemical structures of the polymers and PCBM.

Table 1. Solubility in mg/mL in Different Solvents

	toluene	xylene	mesitylene	$CHCl_3$	chlorobenzene	2-chlorotoluene
PCBM	9	15	29	26	35	47
F8	>100	>100	>100	>100	>100	>100
PFB	>100	>100	>100	>100	>100	>100

were used as substrates for samples analyzed with dynamic SIMS to avoid charging problems. The silicon wafers were cleaned with the RCA standard cleaning method (RCA standard clean 1),[22] which leaves a native thin silicon oxide layer, since otherwise spreading problems were observed during spin-coating.

Solubility. The solubility of PCBM in the different solvents was obtained by equilibrating a solution with an excess of PCBM. A known quantity of supernatant was taken out and the residual weight after solvent evaporation was measured.

Methods. *Spin-Casting.* Films were prepared by spin-coating blend solutions on clean substrates, glass or silica, at 1500 rpm for 80 s with the acceleration set to be immediate.

Three different solvent vapor conditions were used: (a) "No vapor", i.e., no special arrangement to increase the concentration of solvent vapor (open spin-coater). (b) "Medium vapor": The spin-casting was carried out in the presence of extra solvent vapor. This was achieved by having a cylinder of filter paper attached directly on the rotating chuck of the spin-coater as a small chimney, open at the top. The filter paper chimney was soaked with solvent, and the substrate was placed inside. The dimension of the filter paper chimney was 19 mm diameter and 52 mm in height. (c) "High vapor": As for "medium vapor" above but with a plastic lid placed on top to close the opening of the filter paper chimney. The described arrangement made it possible to spin-coat at three different degrees of solvent vapor saturation. If not otherwise indicated, the "no vapor" condition was used.

Surface Energy and Contact Angles. Contact angles using formamide were determined on spin-coated films of pure PCBM and pure polymer, prepared from chloroform solutions (12 mg/mL), using contact angle equipment FTA 200 (First Ten Ångstroms). The contact angles were converted into surface energy values by using the relation by Li and Neumann.[23,24]

AFM. The spin-casted polymer/PCBM films were studied with atomic force microscopy (AFM, NanoScope IIIa, Veeco/Digital Instruments). Tapping mode was used for the morphology imaging. Film thickness was determined using contact mode by measuring the step height across a scratch made in the film.

SIMS. The depth profiles were obtained by a VSW apparatus equipped with liquid metal ion gun (FEI Co.). The sample was sputtered with a Ga^+ primary ion beam of 5 keV (2 nA) over a region 145 × 145 μm, but only the secondary ions from the central 50% part of the sputtered area were collected for analysis. Negatively charged ions were selected and analyzed in a quadrupole mass spectrometer (Balzers); clusters with mass-to-charge ratios (m/q) equal to 24 (corresponding to C_2^-), 26 (corresponding to CN^-), and 28 (corresponding Si^-) were recorded. The CN^- signal is used as a label for the polymer, PFB.[25]

Results and Discussion

Phase Behavior. The phase behavior of three-component, solvent/polymer/PCBM, systems shows two main features. One is a solubility limit of PCBM, in the range of 9−47 mg/mL, depending on the solvent. The second is a two-phase liquid−liquid demixing of the classical type.[26,27] The unusual aspect of this two-phase regime is that it is metastable. The metastable liquid−liquid two-phase regime cannot be studied at equilibrium since it occurs at PCBM concentrations above the solubility limits set by PCBM and is therefore obtained from calculations. This means that with slow solvent evaporation PCBM will nucleate and form crystals before the liquid−liquid phase separation can occur. If a droplet of PCBM (or polymer/PCBM blend) solution evaporates slowly under an optical microscope, formation of micrometer sized PCBM crystals can be seen. A special arrangement with a partly closed sample chamber was needed to reduce the evaporation rate of a 0.5 mL droplet from 10−20 s to 3−4 min for observable crystals (optical microscope) to form. Without the arrangement to reduce the evaporation rate, i.e., 10−20 s evaporation time, crystals were not formed as far as could be judged with optical microscope. The observation that slow evaporation is required for large PCBM crystals (micrometer-sized) to form is in agreement with earlier studies.[28]

However, the metastable two-phase liquid−liquid regime can be accessed by rapid solvent evaporation as will be further discussed in the section on morphology below.

The solubility of PCBM and polymer was obtained as described in the Experimental Section, and values are given in Table 1. As can be seen in Table 1, the polymers (PFB and F8) have a higher solubility than PCBM in the studied solvents.

The liquid−liquid two-phase regions are calculated from Flory−Huggins theory.[26,27] The Flory−Huggins interaction

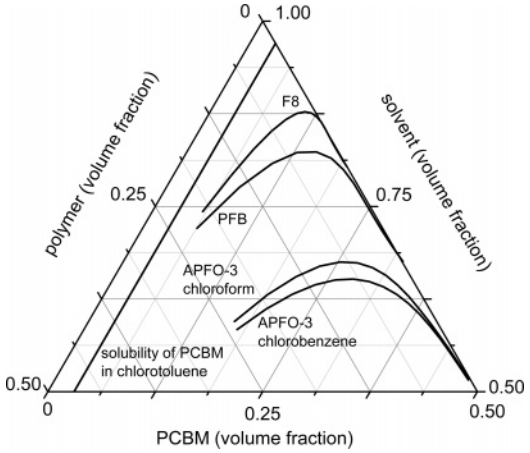

Figure 2. Calculated phase boundaries, binodals, for polymer−PCBM−solvent mixtures with different polymers as indicated (only the upper part of the phase diagram is shown as can be seen from the axes). The effect of solvent is shown for APFO-3; the other polymer curves are calculated with chloroform as solvent. The equilibrium solubility limit of PCBM in chlorotoluene is indicated (conversion from mg/mL to volume fraction was made using density data of PCBM[29] and chlorotoluene). For the other solvents the solubility is lower (see Table 1). The solubility of PCBM should decrease at increasing polymer concentration. However, this effect is small and of little relevance in this context. Note also that only the top section of the full three-phase triangle is shown. At the point labeled 0.25 on the PCBM axis there is therefore 50% solvent, 25% PCBM, and 25% polymer; i.e., the PCBM/polymer ratio is 1:1.

parameters (and solubility parameters) are calculated from experimentally measured contact angles. This somewhat indirect method to obtain interaction parameters was used due to the limited amount of available material. A phase diagram is presented in Figure 2. The interaction parameters and how to calculate phase diagrams as well as the procedure to convert from contact angles to interaction parameters are presented in the Appendix.

The important result from the phase calculations is that the metastable liquid−liquid two-phase region is only weakly dependent on the solvent (shown for APFO-3 in chloroform and chlorobenzene in Figure 2). A large effect comes from which polymer PCBM interacts with. The reason for this is that the two-phase region is mainly determined by the interaction between the polymer and PCBM. Of the present polymers F8 has the lowest surface energy, i.e., the largest difference in surface energy compared to PCBM, and exhibits therefore the largest repulsive interaction. (The larger difference in surface energy corresponds to a larger repulsive interaction, as is analyzed in the Appendix.) It therefore takes lower solute concentrations to induce phase separations in PCBM blends with F8 than with APFO-3, which has a less repulsive interaction toward PCBM. This is reflected in the polymer−PCBM interaction parameters χ_{23} listed in Table 4 where a higher value corresponds to a more repulsive interaction. The difference in interactions is due differences in polarity of the polymers. The polarity is due to amine groups in PFB and benzothiadiazole in APFO-3 and F8BT. APFO-3 also has thiophene units.

Note also that binodals are asymmetric with their maxima toward higher PCBM:polymer ratios. This is because the molecular weight of PCBM is much lower than that of the polymers.

Morphology: General Considerations. When the solvent in a dilute polymer/PCBM/solvent blend evaporates slowly, PCBM crystals precipitate when the PCBM concentration reaches the equilibrium solubility limit of PCBM. With slow evaporation there is no sign of any liquid−liquid demixing, and the amount of crystals increases as the evaporation proceeds and the composition of the liquid in equilibrium with the crystals remains on the solubility line in the phase diagram (Figure 2). However, for PCBM to form well-defined crystals very slow evaporation is required.[28] Under the conditions of spin-casting polymer/PCBM blends, directly observable crystals do not form, and it is discussed in the literature if the structure of the spin-casted film is amorphous or a dispersion of nanocrystals.[28,30−35] On subsequent annealing of PCBM films crystal formation has been observed.[31,35] Spin-casted films of PCBM solutions have been found to have density fluctuations on the nanometer scale,[28,30,31,35] referred to as nanocrystals, though the degree of crystallinity is not known. It is the formation of nanocrystalline material rather than well-defined crystals that makes it possible to produce films from pure PCBM solutions by spin-casting, something which otherwise could be a problem with low molecular weight substances.

With rapid solvent evaporation the composition of the liquid phase can reach higher PCBM concentrations beyond the equilibrium solubility limit of PCBM in Figure 2 because it competes advantageously with nucleation and growth of PCBM crystals. In other words, with a highly volatile solvent the kinetics of evaporation is faster then the kinetics of crystallization.

Strong support for the existence of the calculated metastable liquid−liquid two-phase regions is the formation of surface-directed spinodal waves upon spin-casting chloroform solutions of APFO-3/PCBM blends reported in ref 25. Vertical phase separation due to spinodal waves has also been reported for spin-casted films of other systems where the liquid two-phase region is directly accessible at equilibrium.[12,13,49] Spinodal wave formation is a classical mechanism[6] for initiating phase separation in liquid−liquid two- phase regions which shows that the composition of the liquid phase can reach the calculated metastable two-phase regions. In polymer/PCBM systems at equilibrium or system evaporating slowly this would of course be impossible due to the solubility limit set by PCBM.

PFB/PCBM Blends: Effects of Evaporation Rate. From the above reasoning solvent evaporation rates can be expected to have an effect on the morphology for films prepared from spin-coating. This is also what can be seen for both PFB and F8 blends with PCBM. Figures 3 and 4 show the effect of reducing the evaporation rate for PFB/PCBM blends in the case of xylene as solvent. The evaporation rate was reduced by spin-casting in the presence of extra solvent vapor (Figure 4).

As can be seen in the AFM images in Figures 3 and 4, there are quite significant changes in the morphology due to the solvent evaporation rate. Without extra solvent vapor the film with 1:1 blend ratio is rather flat and featureless. While at increasing PCBM contents (blend ratio 1:2−1:4) island formation is clearly seen. The same kind of island formation for PFB/PCBM blends has also been observed previously with chloroform as solvent.[40] One difference is that with chloroform islands were formed also with blend ratio of 1:1.

When solvent vapor is used to reduce the evaporation rate during spin-casting, the films become flatter (note the height scale) than was the case without extra solvent vapor. The blend ratio 1:2 now gives an almost completely flat surface; at higher blend ratios (1:3 and 1:4) there is some lateral structure but much more diffuse. The surfaces (1:3 and 1:4) have also become more flattened with a reduced vertical height difference. The "flattening" is quantified in Figure 5 as the root-mean-square

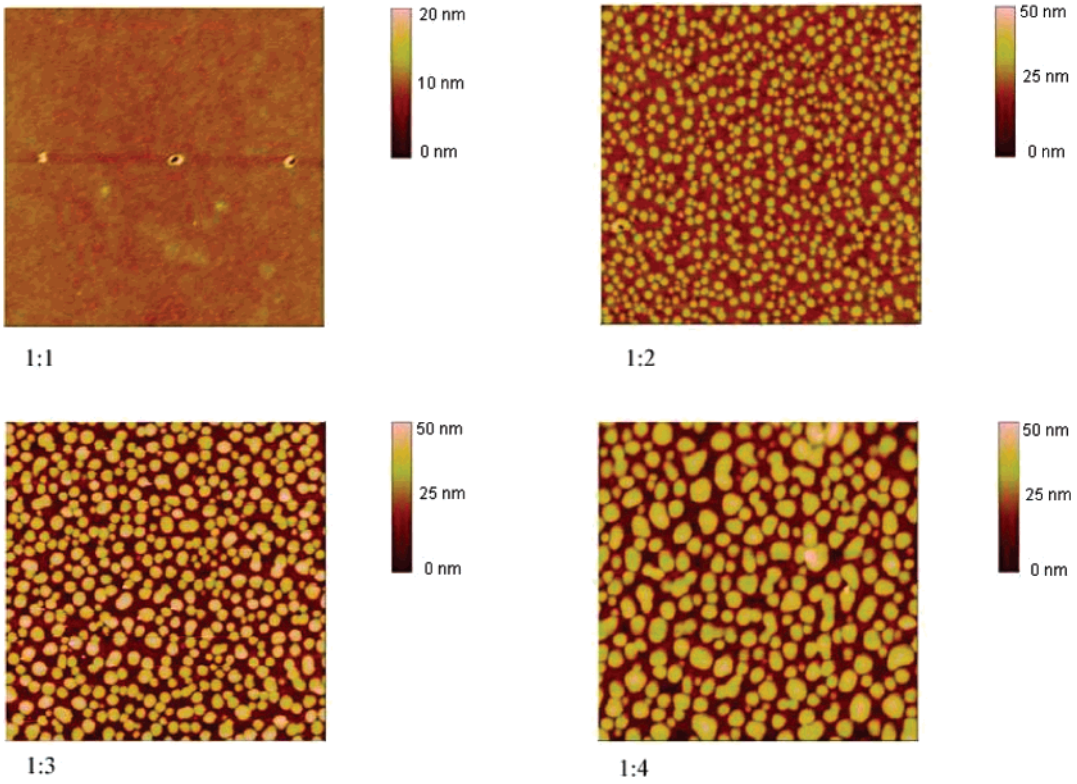

Figure 3. AFM height images (5 μm × 5 μm) of spin-casted PFB/PCBM blends from xylene under "no vapor" conditions. The blend ratios are indicated.

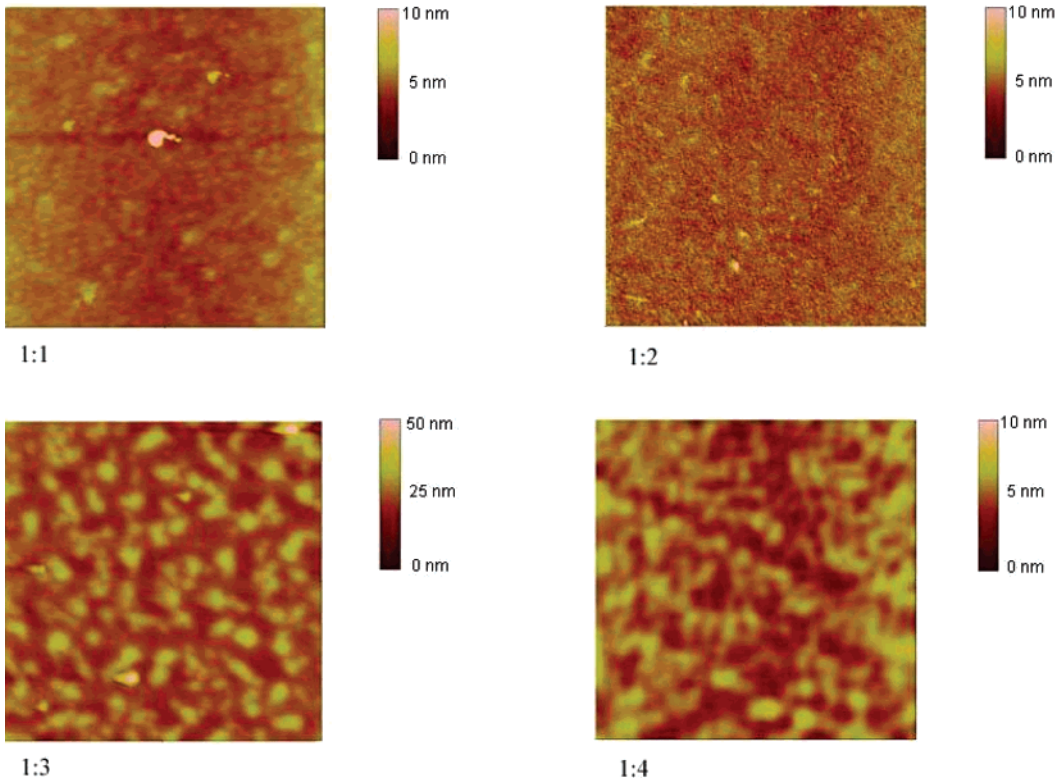

Figure 4. AFM height images (5 μm × 5 μm) of spin-casted PFB/PCBM blends from xylene under "high vapor" conditions. Blend ratios are indicated. The evaporation rate was reduced by producing an atmosphere with high vapor content around the sample.

roughness for the different blend ratios and evaporation rates. The film thickness is 18 nm for high vapor and 31 nm for no vapor conditions and depends only marginally on the blend ratio.

With medium vapor condition during spin-coating, islands are formed (AFM images not shown) at a blend ratio of 1:2, but the trend toward a flatter surface structure is rather clear (Figure 5).

The trend deduced from these data is that reduced evaporation rate causes a transition from a lateral surface structure with high roughness to a flat surface. A possible interpretation of these

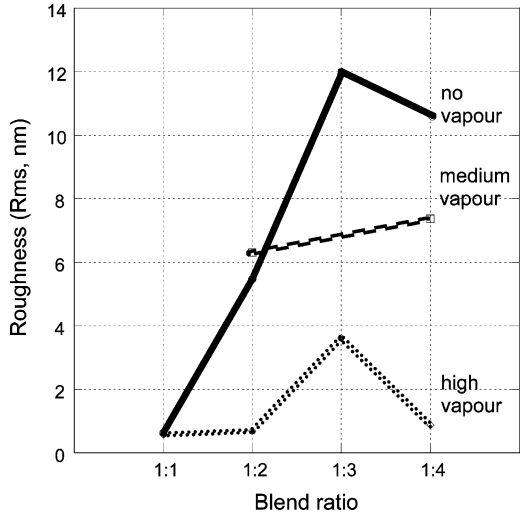

Figure 5. Surface roughness for spin-casted PFB/PCBM blends from xylene as a function of blend ratio (polymer/PCBM) and evaporation rates (vapor conditions during spin-casting), as indicated.

results is that this is caused by the balance between the rate of liquid−liquid phase separation and also the kinetics of PCBM crystallization (in the form of nanocrystals) governed by the rate of solvent evaporation.

Polymer Effect: Comparison of PFB, F8, and APFO-3. With higher evaporation rates the composition of the liquid phase can reach the liquid−liquid two-phase region as discussed above. When the liquid composition comes deep enough into the liquid−liquid two-phase region, i.e., larger quench depth, phase separation can be initiated by spinodal waves. When a system is solvent quenched into a two-phase region phase, instability occurs earlier at surfaces and then in bulk,[38] and spinodal waves are therefore often surface directed. Structure formation models suggest initial formation of multilayers which can either be frozen in or break up to form lateral structures.[9,10,39]

This depends on the strength of polymer−PCBM interaction parameter governing interfacial energy. With large enough interfacial energy between the phases (rich in polymer and PCBM) the layers would be unstable and hence break up into islands. The island formation must of course take place before the system is frozen due to solvent evaporation. With the weakly repulsive APFO-3/PCBM blend in $CHCl_3$ the result was multilayers.[25] PFB/PCBM (in $CHCl_3$)[40] exhibits a stronger repulsive interaction and produced islands that are somewhat diffuse, and finally F8/PCBM (in $CHCl_3$) with the strongest repulsive interaction gave quite distinct island formation.[40] Stronger polymer−PCBM interactions result in interfacial instabilities with larger wavelength and finally with larger lateral structures.[50]

A schematic illustration is given in Figure 6. The lamellar−lateral structure transition observed here in solvent-quenched blend series is analogous to the plating−droplet (wetting) transition reported earlier for temperature-equilibrated polymer blends.[51,52] The sequence APFO-3 < PFB < F8 for the repulsive interaction with PCBM can be seen both in the phase diagram (Figure 2) and in the χ_{23} parameters in Table 4.

On the basis of the above reasoning, the following scheme can be anticipated for spin-casted polymer/PCBM films. At high evaporation rates surface directed spinodal waves are initiated by quenching into the liquid two-phase region. The lamellar structure formed by spinodal waves can be frozen in or broken up into islands depending on the interfacial energies.

If the rate of evaporation is reduced by solvent vapor during the spin-coating, the composition of the liquid phase cannot come as deep into the liquid two-phase region before onset of liquid-phase separation or may not reach it at all before the competing kinetics of PCBM crystallization becomes significant. Reduced evaporation rates correspond to a reduced quench depth or less solute concentration buildup before the system has time to respond by phase separation. This will make the formation of spinodal waves less likely.

If the evaporation is slow enough, the composition of the liquid phase cannot reach the liquid two-phase region at all due to PCBM crystallization. Since PCBM crystals produced during spin-casting are nanometer-sized, on the basis of literature data as discussed in the general section above, the likely result would be nanometer-sized aggregates or crystals dispersed in a polymer solution. The result of such a process should be a film which is quite homogeneous both laterally and vertically. This aspect is a rather special feature for PCBM.

For a polymer/PCBM system with weak repulsion, e.g., APFO-3/PCBM, it takes a higher evaporation rate to build up the concentration to reach the liquid two-phase region fast enough (before PCBM crystallization takes over) than for a system with stronger repulsion, e.g., with PFB or F8. This is seen in Figure 2 from the fact that binodals for APFO-3 are located at higher solute concentrations than the ones for F8 and PFB.

PFB/PCBM Blends: Effect of Solvent. To see how well the suggested mechanism agrees with experimental data, different polymer/PCBM/solvent combinations have been investigated. Solvent properties are summarized in Table 2 (vapor pressure data are taken from ref 41 and solubility parameter data from ref 42). With the rapidly evaporating chloroform, as has already been mentioned, PFB/PCBM blends give a lateral island structure. Toluene as a solvent, which is less volatile then $CHCl_3$ and close to xylene in vapor pressure (see Table 2), results in a morphology similar to the one of PFB/PCBM blends in xylene (Figure 7).

The reason why a higher blend ratio favors island formation with toluene and xylene as solvents can be understood from

Table 2. Solvent Properties Listed in Order of Decreasing Vapor Pressure and Resulting Morphology of Spin-Casted PFB/PCBM Blends for These Solvents with Different Vapor Pressures (Blend Ratios Are As Indicated)

	solubility parameter, $(cal/cm^3)^{1/2}$	vapor pressure at 25 °C (kPa)	morphology for blend ratio 1:1	morphology for blend ratio 1:4
$CHCl_3$ (ref 40)	9.3	26.2	lateral	lateral
toluene[a]	8.9	3.8	flat	lateral
chlorobenzene	9.5	1.6	flat	flat
xylene	8.8	1.1	flat	lateral
2-chlorotoluene[b]	9.6	0.48	flat	flat
mesitylene	8.8	0.33	flat	flat

[a] The blend ratios with toluene was 1:1 and 1:3. [b] The solubility parameter of 2-chlorotoluene was calculated using Hoy's group contribution method to ortho-substitute toluene with chlorine, yielding a value of 9.6.

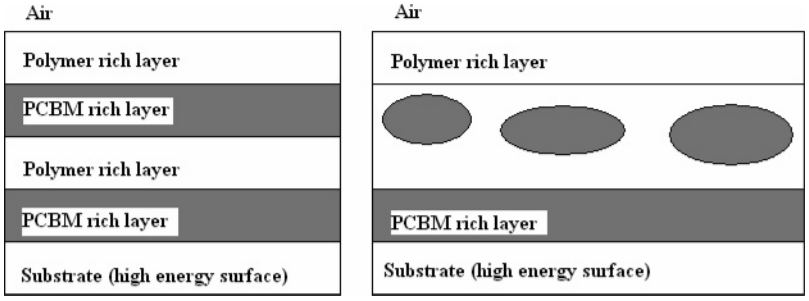

Figure 6. Schematic drawing illustrating the formation of islands or droplets (right) as a breakup of spinodally formed multi layers (left).

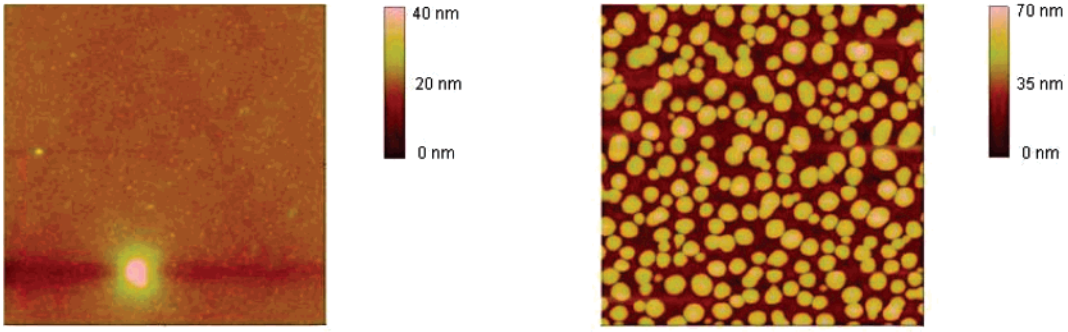

Figure 7. AFM height images (5 μm × 5 μm) of spin-casted PFB/PCBM blends from toluene. Blend ratios are as indicated. (Because of the limited solubility of PCBM in toluene, the highest blend ratio that could be prepared in this case is 1:3.)

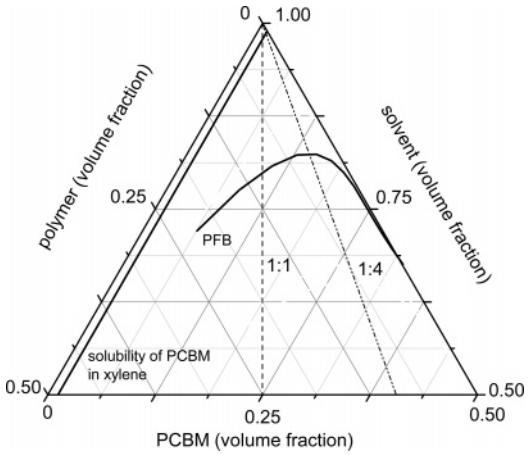

Figure 8. Calculated phase boundary, binodal, for PFB−PCBM−xylene (only the upper part of the phase diagram is shown as can be seen from the axes). The dashed line indicates a 1:1 PFB/PCBM blend ratio and the dot-dashed line a 1:4 ratio.

the phase diagram. The distance measured in solvent content from the starting point (a 12 mg/mL solution) to the liquid two-phase boundary is larger at blend ratio 1:1 than for a 1:4 ratio (see Figure 8).

For a 1:4 blend ratio 16% of the solvent needs to evaporate before the total composition reaches the liquid two-phase boundary. For solutions with 1:1 blend ratio, 19% of the solvent needs to evaporate to reach the phase boundary. This will take longer time. A 1:1 blend ratio allows therefore more time for the competing kinetic processes discussed above, and as a result it is easier to suppress lateral structures with extra solvent vapor during spin-casting than for a 1:4 blend. Larger islands observed for blend composition closer to its critical value might indicate lateral phase separation effective after layer instabilities.[8]

Other solvents with different volatilities have also been examined. The change from chloroform to toluene and xylene has already been mentioned above. Turning to mesitylene, which is chemically similar to xylene but less volatile, results in a flat surface structure for PFB/PCBM blends with ratios 1:1 and 1:4 (Figure 9).

Changing to more polar solvents like chlorobenzene and 2-chlorotoluene (see Table 2) gives flat surface structures for PFB/PCBM blends with ratios 1:1 and 1:4 (data not shown since the AFM height images for PFB/PCBM blends using chlorobenzene or 2-chlorotoluene as solvents have almost exactly the same appearance as in Figure 9).

The flat surface with 2-chlorotoluene is expected on the basis of the low vapor pressure. With chlorobenzene the situation is a little different. The morphology is a flat surface for both PFB/PCBM 1:1 and 1:4 blends for spin-casting from chlorobenzene. Since a 1:4 blend spin-casted from xylene gives an island structure, one would expect a similar lateral structure in chlorobenzene, since chlorobenzene is more volatile than xylene (as judged from the vapor pressure, Table 2). On the other hand, PFB blends from xylene gives a flat structure for a 1:1 blend and islands with a 1:4 blend which shows that the vapor pressure of xylene is close to the transition between giving only lateral or only flat surface structures. The difference in vapor pressure between xylene and chlorobenzene is small compared to the other solvents, and though evaporation rate is an important factor it is of course not the only factor. Differences in solubility and precise location of phase boundaries and perhaps also the viscosity contribution from dissolved polymer, which might be different in the two solvents, may play a role though evaporation rate seems to dominate. In the case of APFO-3, changing solvent from chloroform to chlorobenzene changes the structure from multilayer to homogeneous as is in the expected direction.[43]

The resulting morphology for spin-casted PFB/PCBM blends is summarized in Table 2 in order of decreasing solvent vapor pressure. The morphology is described as “lateral” or “flat”. As has been discussed above, chlorobenzene is somewhat out of place but the correlation between type of morphology and solvent vapor pressure is rather clear. We may note that the

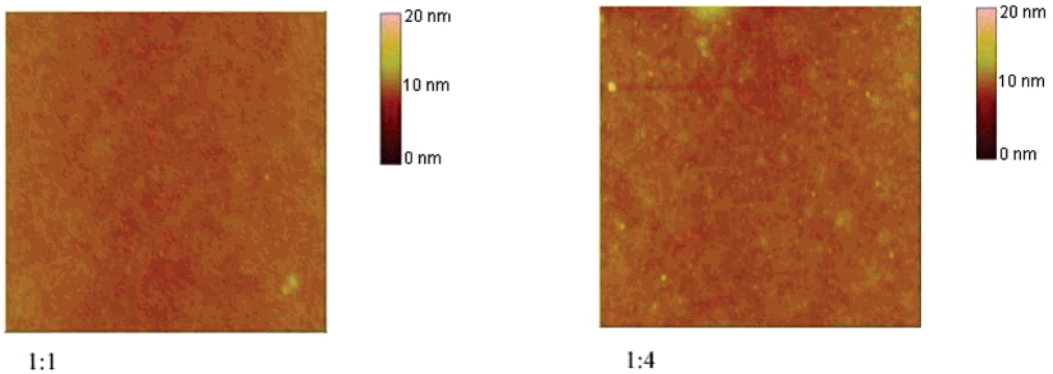

Figure 9. AFM height images (5 μm × 5 μm) of spin-casted PFB/PCBM blends from mesitylene. Blend ratios are as indicated.

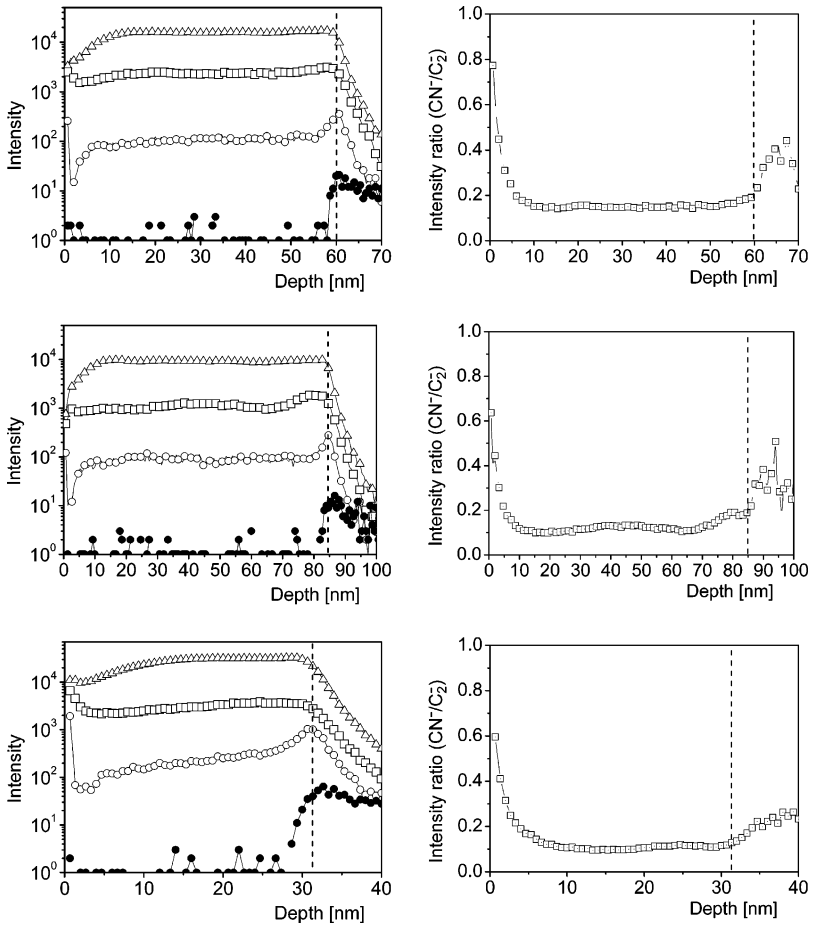

Figure 10. Intensity vs depth of negative ions obtained by SIMS sputtering of spin-casted films of PFB/PCBM (1:4). In the left column, intensity vs depth profiles for C_2^- (open triangles), CN^- (open squares), O^- (open circles), and Si^- (filled circles) are shown. In the right column the CN^-/C_2^- ratio vs depth is presented. The systems are from top to bottom, PFB/PCBM (1:4) films spin-coated from a 30 mg/mL solution in 2-chlorotoluene, from a 30 mg/mL solution in chlorobenzene, and from a 12 mg/mL solution in chlorobenzene.

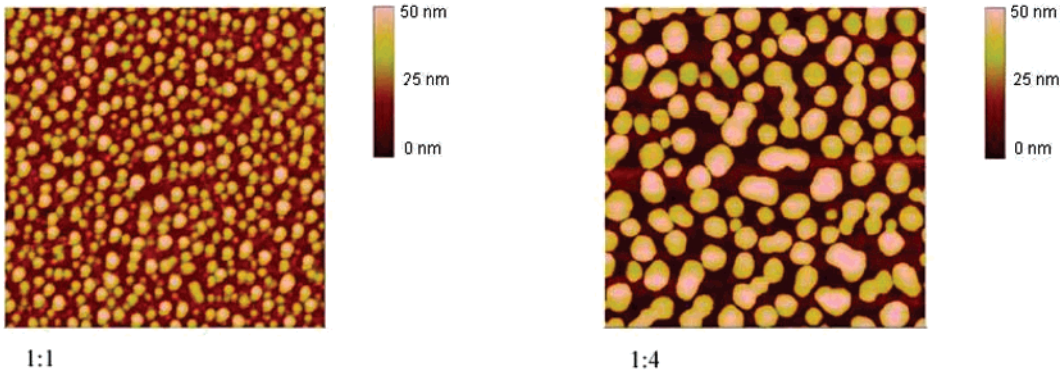

Figure 11. AFM height images (5 μm × 5 μm) of spin-casted F8/PCBM blends from xylene; blend ratios as indicated.

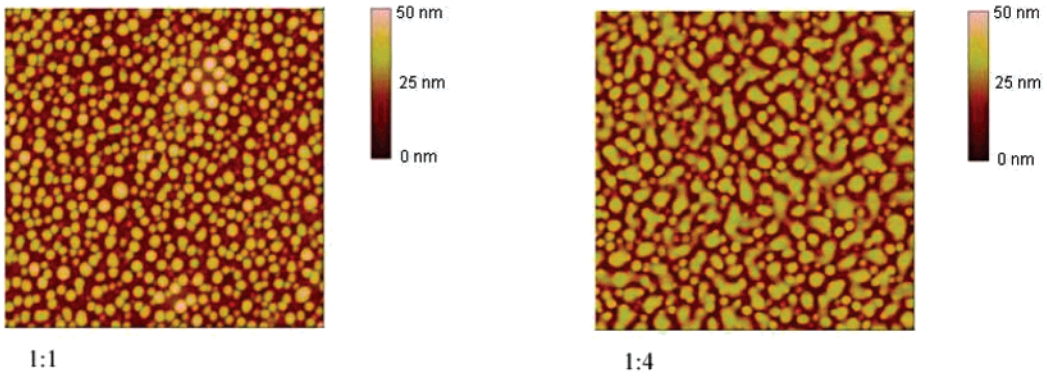

Figure 12. AFM height images (5 μm × 5 μm) of spin-casted F8/PCBM blends from chlorobenzene; blend ratios as indicated.

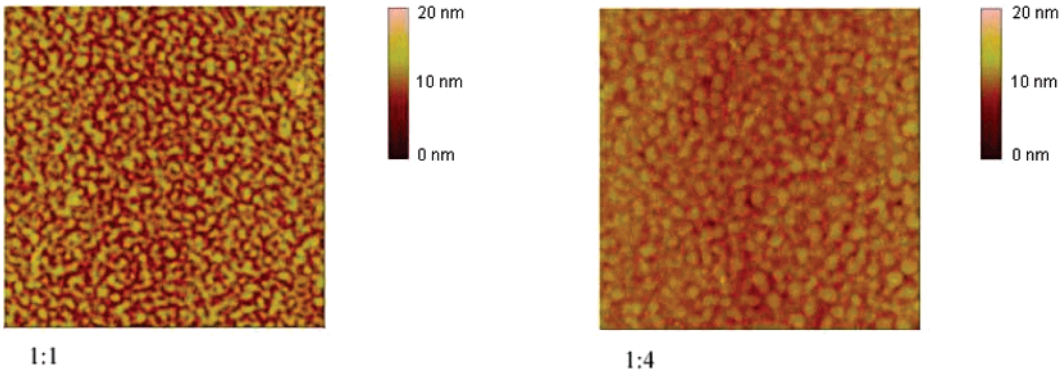

Figure 13. AFM height images (5 μm × 5 μm) of spin-casted F8/PCBM blends from 2-chlorotoluene; blend ratios as indicated.

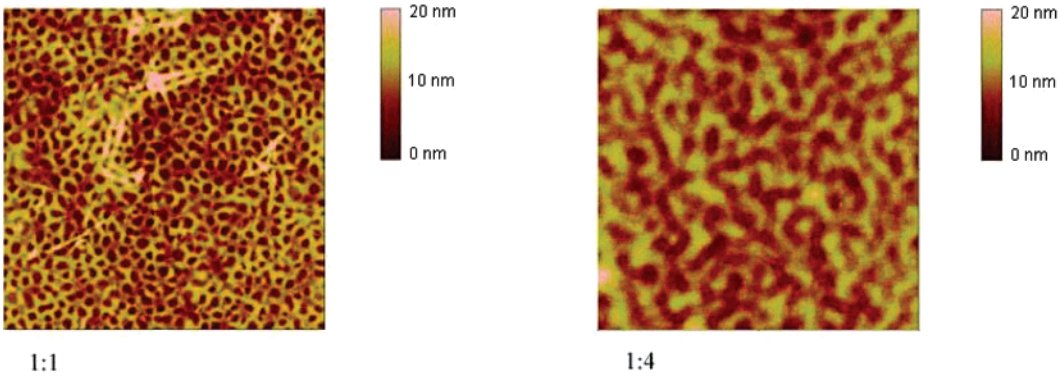

Figure 14. AFM height images (5 μm × 5 μm) of spin-casted F8/PCBM blends from mesitylene; blend ratios as indicated.

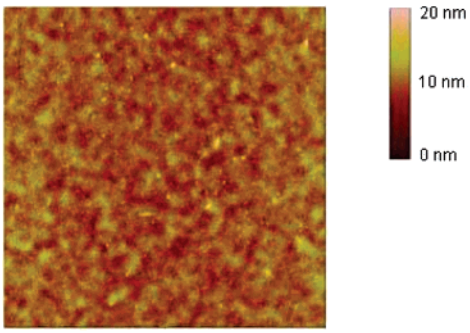

Figure 15. AFM height images (5 μm × 5 μm) of spin-casted F8/PCBM 1:1 blend spin-casted with "high vapor" conditions.

different solubilities of PCBM and polymer in the different solvents do not seem to be a main factor.

The flat surface structures revealed in the AFM pictures above gives of course no information about the vertical structure. Dynamic SIMS studies have therefore been carried out for some samples to verify whether the films were homogeneous or layered. A typical result is shown in Figure 10 for PFB/PCBM films spin-casted from 2-chlorotoluene.

The results presented in Figure 10 show a rather homogeneous distribution of PFB (CN^- signal) throughout the films. The initial variation in the signals is caused by the sputtering rate that needs stabilize before reaching steady state. The PCBM composition cannot be followed since there is no suitable label in the PCBM molecule for SIMS, but since there is little variation in the polymer composition, it can be assumed that there is little variation for PCBM as well. The thickness of films prepared from 12 mg/mL solutions is 26−30 nm, which is at the lower limit of what is suitable for dynamic SIMS. Depth resolution in dynamic SIMS is about 10 nm.[44] Thicker films were therefore also made by spin-coating 30 mg/mL solutions (the films from the 30 mg/mL solutions were about 70 nm thick) and analyzed by SIMS. Even though the C_2^- signal is not at steady state in the initial part it can be seen from the ratio of CN^-/C_2^- (Figure 10, right column) that there seems to be a surface enrichment of polymer.

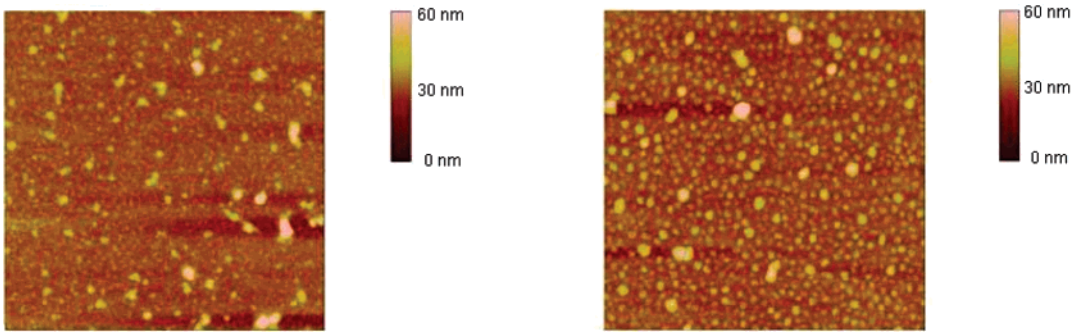

Figure 16. AFM height images (5 μm × 5 μm) of 1:1 blend of F8/F8BT spin-casted from toluene (left) and xylene (right).

Table 3. Contact Angle (Formamide), Surface Energies, and Solubility Parameters for the Indicated Polymers

	contact angle, deg	surface energy, mN/m	solubility parameter, $(cal/cm^3)^{1/2}$
F8	81	25.3	9.2
PFB	77	27.1	9.5
F8BT	73	29.6	10.0
APFO-3	68	32.2	10.4
PCBM	57	37.8	11.3

Table 4. Flory−Huggins Interaction Parameters for Polymer/PCBM in Different Solvents[a]

	χ_{12}	χ_{13}	χ_{23}
$CHCl_3$/F8/PCBM	0.341	0.885	0.941
chlorobenzene/F8/PCBM	0.356	0.899	1.100
chlorobenzene /PFB/PCBM	0.340	0.899	0.899
$CHCl_3$/APFO-3/PCBM	0.505	0.885	0.450
chlorobenzene /APFO-3/PCBM	0.480	0.899	0.479
xylene/PFB/PCBM	0.442	1.630	1.013

[a] Indices: 1 = solvent, 2 = polymer, and 3 = PCBM.

Table 5. Degree of Polymerization

	N		*N*
F8	720	APFO-3	66
PFB	73	PCBM	5
F8BT	172		

SIMS analysis was also carried out for other blend ratios (1:1 and 1:4) and solvents (xylene, chlorobenzene, chlorotoluene, and mesitylene) using 12 mg/mL solutions and 1:4 blends in chlorobenzene, chlorotoluene, and mesitylene using 30 mg/mL. However, the result was similar to what can be seen in Figure 10, and the data are therefore not shown. The finding that the flat surface structures observed with AFM are not only flat but also homogeneous in the vertical directions is in good agreement with the suggested mechanisms, i.e., the formation of nanosized crystals or aggregates dispersed in a polymer matrix.

F8/PCBM Blends. For F8, which has a more repulsive interaction with PCBM than PFB, the morphology for spin-casted films is island formation in all the studied solvents in using "no vapor" conditions. Chloroform (ref 40), xylene, mesitylene chlorobenzene, and 2-chlorotoluene all give lateral structures (Figures 11−14).

From the above interpretation it is to be expected that F8/PCBM blends give lateral structures at much lower evaporation rates than the other polymers. One aspect that can be noted and which has not been discussed before is that different lateral structures form in the different solvent. This is probably related to exactly how an initial multilayer structure breaks up into lateral domain (see Figure 6); viscosities may perhaps play a role. The details on how the lateral domains form are however beyond the scope of the present study.

Investigating the effect of reducing the evaporation rate, selecting mesitylene, the slowest evaporating solvent, it can again be seen that the structure tends to a flat surface (Figure 15) even for F8/PCBM.

The behavior of polymer/PCBM blends can be contrasted against a system where the liquid−liquid two phase region is accessible also at equilibrium, i.e., where the liquid−liquid two phase region is not perturbed by a solubility limit of the components. One such system is the blend of F8/F8BT where both components have high solubility in the solvents used.

As can be seen in Figure 16, larger domains are formed with the more slowly evaporating xylene compared to toluene as solvent. This is simply because slower evaporation gives more time for the lateral domains to grow and develop and is what one usually would expect for polymer/polymer blends. The same trend as in Figure 16 of increasing domain size with less volatile solvents on spin-casting "simple" polymer−polymer blends has also been observed earlier.[45]

Conclusions

It has been found that the main parameters that determine the morphology of spin-casted films of polymer/PCBM blends are the evaporation rate which can be tuned by choice of solvent or by spin-coating or controlling vapor atmosphere and the polymer−PCBM interaction. Lateral structure formation is favored by rapid evaporation and strong polymer−PCBM repulsion. Homogeneous structures are favored by less volatile solvents and weak polymer−PCBM repulsion. Normally, i.e., for polymer/polymer blends, it would be expected that a slow evaporation gives more time for structure development, as is indeed also what is seen for polymer/polymer blends.

The contrasting behavior of the polymer/PCBM blend is explained by a limited solubility of PCBM in combination with a slow kinetics of crystallization. The slow kinetics of crystallization makes it possible to quench the system, by rapid solvent evaporation, beyond the equilibrium solubility limit into a metastable region with classical polymer−polymer two-phase incompatibility. How deep the quenching goes into the metastable two-phase region is controlled by the evaporation rate and the precise location of the two-phase region. The location of the metastable two phase region is governed by the polymer−PCBM interaction and thus the structure of the polymer. A deep quench into the metastable two-phase region, which is of the liquid−liquid type, gives rise to lateral structure formation, typically as "islands". Shallow solvent quenching, slow evaporation, results in nanosized aggregates or crystals dispersed in a polymer matrix, the result of which is more or less homogeneous.

Acknowledgment. The authors thank Prof. Mats R. Andersson, Polymer Technology, Chalmers University of Technology, Göteborg, Sweden, for generously providing APFO-3. The Swedish Research Council is acknowledged for financial support

(Contract 621-2002-4694). A. Bernasik is grateful for financial support from the Polish State Committee for Scientific Research.

Appendix. Interaction Parameters

Interaction parameters in the Flory−Huggins model are usually obtained by thermodynamic methods like osmotic pressure or direct fitting to the observed phase diagram. Because of the limited amounts of available polymer material and also of course the metastable nature of the liquid demixing regime, a different approach was used.

Surface energies were obtained by measuring contact angles on spin-casted surfaces prepared from chloroform solutions of the pure components (12 mg/mL). The measured contact angles were converted to surface energies using the relation by Li and Neumann.[23,24] With formamide as test liquid the resulting contact angles and surface energies are shown in Table 3.

Surface energy (γ) gives the interaction per unit area with the interaction parameter (χ) between two components being proportional to[26,48]

$$\chi_{ij} \propto (\sqrt{\gamma_i} - \sqrt{\gamma_j})^2 \tag{A1}$$

What is needed in the Flory−Huggins model is the interaction per lattice site; the difference in molecular size is then taken care of by the degree of polymerization. To determine the proportionality factor between interaction parameter and surface energy, advantage has been taken of the fact that the solubility parameter of polymer F8 is known experimentally.[46]

The solubility parameter (δ) for F8 has from turbidity been determined[46] to be in the range 9.1−9.3 $(\text{cal/cm}^3)^{1/2}$. Since solubility parameters are proportional to the square root of the surface energy, the same proportionality was used for all components giving the solubility parameters listed in Table 3. Using the same proportionality means that possible effects from variations in segment volume of the repeating units are ignored. However, since the square of the solubility parameter is proportional to cubic root[42] of the volume, the effect is not critical. The relative ordering between the blend components (polymer and PCBM) is given by eq A1, and as is emphasized below, it is the relative ordering between the components that is important here.

The χ parameters are then calculated from the solubility parameters by the relation[42]

$$\chi_{ij} = \frac{V_1}{RT}(\delta_i - \delta_j)^2 + 0.34 \tag{A2}$$

where V_1 is the molar volume of the solvent, which defines the unit lattice size. The term 0.34 gives the entropic contribution and is usually between 0.3 and 0.4 for nonpolar systems; 0.34 is often used.[42] However, the precise value adopted is not critical.

A list of χ parameters with some solvents is shown in Table 4. (Solubility parameters for the solvents are taken from the literature[42] and listed in Table 2.)

The conversion from contact angles to interaction parameters is of course an approximation. However, what is important in this context is the relative ranking or ordering between the components rather than precise numerical values. This is especially so considering that the use of solubility parameters to describe thermodynamic properties is in itself an approximation. The main purpose here is to understand the trends when varying different parameters.

The remaining factors in the Flory−Huggins model are the degrees of polymerization. The molecular weight is 140 000 for F8, 10 000 for PFB, 30 000 for F8BT, and 11 800 for APFO-3. This gives the number of repeating units for F8 as 360. Taking a solvent molecule like chlorobenzene as the unit size and with two aromatic rings per repeating unit for F8 gives the degree of polymerization as 720. The values for the other polymers are obtained analogously counting the number of rings along the polymer chain and are listed in Table 5.

PCBM is not a polymer but a rather large molecule. The molar volume is ca. 600 cm^3/mol (based on the density, ref 29), which is about 5−6 times the volume of the solvent molecules. The precise values in Table 5 for either polymer or PCBM are not critical for the qualitative behavior.

The expression for the free energy, G, in the Flory−Huggins model[26,27] is

$$G/RT = n_{\text{tot}}\left(\phi_1 \ln \phi_1 + \frac{\phi_2}{N_2}\ln \phi_2 + \frac{\phi_3}{N_3}\ln \phi_3 + \chi_{12}\phi_1\phi_2 + \chi_{13}\phi_1\phi_3 + \chi_{23}\phi_2\phi_3\right) \tag{A3}$$

where ϕ_i is the volume fraction of component i, the indices refer to 1 = solvent, 2 = polymer, and 3 = PCBM, as before.

Chemical potentials are obtained by differentiation of the free energy expression in the usual manner.[26,27] An efficient and practical algorithm for how to construct a three-component phase diagram from chemical potentials is described elsewhere.[47]

References and Notes

(1) Nelson, J. *Curr. Opin. Solid State Mater. Sci.* **2002**, *6*, 87.
(2) Gebeyehu, D.; Brabec, C. J.; Padinger, F.; Fromherz, T.; Hummelen, J. C.; Badt, D.; Schindler, H.; Sariciftci, N. S. *Synth. Met.* **2001**, *118*, 1.
(3) van Duren, J. K. J.; Yang, X.; Loos, J.; Bulle-Lieuwma, C. W. T.; Sieval, A. B.; Hummelen, J. C.; Janssen, R. A. J. *Adv. Funct. Mater.* **2004**, *14*, 425.
(4) Shaheen, S. E.; Brabec, C. J.; Sariciftci, N. S.; Padinger, F.; Fromherz, T.; Hummelen, J. C. *Appl. Phys. Lett.* **2001**, *78*, 841.
(5) Martens, T.; D'Haen, J.; Munters, T.; Beelen, Z.; Goris, L.; Manca, J.; D'Olieslaeger, M.; Vanderzande, D.; De Schepper, L.; Andriessen, R. *Synth. Met.* **2003**, *138*, 243.
(6) Jones, R. A. L.; Richards, R. W. *Polymers at Surfaces and Interfaces;* Cambridge University Press: New York, 1999.
(7) Jukes, P. C.; Heriot, S. Y.; Sharp, J. S.; Jones, R. A. L. *Macromolecules* **2005**, *38*, 2030.
(8) Budkowski, A.; Bernasik, A.; Cyganik, P.; Raczkowska, J.; Penc, B.; Bergues, B.; Kowalski, K,.; Rysz, J.; Janik, J. *Macromolecules* **2003**, *36*, 4060.
(9) Sprenger, M.; Walheim, S.; Budkowski, A.; Steiner, U. *Interface Sci.* **2002**, *11*, 225.
(10) Raczkowska, J.; Bernasik, A.; Budkowski, A.; Sajewicz, K.; Penc, B.; Lekki, J.; Lekka, M.; Rysz, J.; Kowalski, K.; Czuba, P. *Macromolecules* **2004**, *37*, 7308.
(11) Ton-That, C.; Shard, A. G.; Teare, D. O. H.; Bradley, R. H. *Polymer* **2001**, *42*, 1121.
(12) Geoghegan, M.; Jones, R. A. L.; Payne, R. S.; Sakellariou, P.; Clough, A. S.; Penfold, J. *Polymer* **1994**, *35*, 2019.
(13) Bernasik, A.; Wlodarczyk-Miskiewicz, J.; Luzny, W.; Kowalski, K.; Raczkowska, J.; Rysz, J.; Budkowski, A. *Synth. Met.* **2004**, *144*, 253.
(14) Higgins, A. M.; Martin, S. J.; Thompson, R. L.; Chappell, J. C.; Voight, M.; Lidzey, D. G.; Jones, R. A. L.; Geoghegan, M. *J. Phys.: Condens. Matter* **2005**, *17*, 1319.
(15) Arias, A. C.; Corcoran, N.; Banach, M.; Friend, R. H.; MacKenzie, J. D.; Huck, W. T. S. *Appl. Phys. Lett.* **2002**, *80*, 1695.
(16) Chappell, J.; Lidzey, D. G.; Jukes, P. C.; Higgins, A. M.; Thompson, R. L.; O'Connor, S.; Grizzi, I.; Fletcher, R.; O'Brien, J.; Geoghegan, M.; et al. *Nat. Mater.* **2003**, *2*, 616.
(17) Voigt, M.; Chappell, J.; Rowson, T.; Cadby, A.; Geoghegan, M.; Jones, R. A. L.; Lidzey, D. G. *Org. Electron.: Phys. Mater. Appl.* **2005**, *6*, 35.
(18) Kim, J-S.; Ho, P. K. H.; Murphy, C. E.; Friend, R. H. *Macromolecules* **2004**, *37*, 2861.
(19) Chua, L-L.; Ho, P. K. H.; Sirringhaus, H.; Friend, R. H. *Adv. Mater.* **2004**, *16*, 1609.

(20) Boltau, M.; Walheim, S.; Mlynek, J.; et al. *Nature (London)* **1998**, *391*, 877.
(21) Walheim, S.; Boltau, M.; Mlynek, J.; Krausch, G.; Steiner, U. *Macromolecules* **1997**, *30*, 4995.
(22) Kern, W. *J. Electrochem. Soc.* **1990**, *137*, 1887.
(23) Li, D.; Neumann, A. W. *J. Colloid Interface Sci.* **1990**, *137*, 304.
(24) Li, D.; Neumann, A. W. *J. Colloid Interface Sci.* **1992**, *148*, 190.
(25) Björström, C.; Bernasik, A.; Rysz, J.; et al. *J. Phys.: Condens. Matter* **2005**, *17*, L529.
(26) Flory, P. *Principles of Polymer Chemistry*; Cornell University Press: Ithaca, NY, 1953.
(27) Scott, R. L. *J. Chem. Phys.* **1949**, *17*, 279.
(28) Yang, X.; van Duren, J. K. J.; Rispens, M. T.; et al. *Adv. Mater.* **2004**, *16*, 802.
(29) Bulle-Lieuwma, C. W. T.; van Gennip, W. J. H.; van Duren, J. K. J.; et al. *Appl. Surf. Sci.* **2003**, *203*, 547.
(30) Yang, X.; Loos, J.; Veenstra, S. C.; et al. *Nano Lett.* **2005**, *5*, 579.
(31) Yang, X.; van Duren, J. K. J.; Janssen, R. A. J.; et al. *Macromolecules* **2004**, *37*, 2151.
(32) Erb, T.; Zhokhavets, U.; Gobsch, G.; et al. *Adv. Funct. Mater.* **2005**, *15*, 1193.
(33) Erb, T.; Zhokhavets, U.; Hoppe, H.; et al. *Thin Solid Films*, in press.
(34) Zhokhavets, U.; Erb, T.; Hoppe, H.; et al. *Thin Solid Films* **2006**, *496*, 679.
(35) Hoppe, H.; Drees, M.; Schwinger, W.; et al. *Synth. Met.* **2005**, *152*, 117.
(36) Raczkowska, J.; Rysz, J.; Budkowski, A.; et al. *Macromolecules* **2003**, *36*, 2419.
(37) Affrossman, S.; Henn, G.; O', Neill, S. A.; et al. *Macromolecules* **1996**, *29*, 5010.
(38) Nilsson, S.; Linse, P. *J. Chem. Phys.* **1993**, *99*, 2167.
(39) Heriot, S. Y.; Jones, R. A. L. *Nat. Mater.* **2005**, *4*, 782.
(40) Björström, C. M.; Moons, E.; Magnusson, K. O. *Synth. Met.* **2005**, *152*, 109.
(41) *Handbook of Chemistry and Physics*, 76th ed.; Lide, D. R., Ed.; CRC Press: Boca Raton, FL, 1995−1996.
(42) *Polymer Handbook*, 4th ed.; Brandrup, J., Immergut, E. H., Grulke, E. A., Eds.; John Wiley & Sons: New York, 1999.
(43) Björström, C. M.; Nilsson, S.; Magnusson, K. O.; Moons, E.; Bernasik, A.; Rysz, J.; Budkowski, A.; Zhang, F.; Inganäs, O.; Andersson, M. R.; *Proceedings of the SPIE Conference*, Photonics Europe 2006: Photonics Applications.
(44) Bernasik, A.; Rysz, J.; Budkowski, A.; et al. *J. Macromol. Rapid Commun.* **2001**, *22*, 829.
(45) Moons, E. *J. Phys.: Condens. Matter* **2002**, *14*, 12235.
(46) Grell, M.; Bradley, D. D. C.; Long, X. *Acta Polym.* **1998**, *49*, 439.
(47) Hellebust, S.; Nilsson, S.; Blokhus, A. M. *Macromolecules* **2003**, *36*, 5372.
(48) Israelachvili, J.N. *Intermolecular and Surface Forces*; Academic Press: London, 1992.
(49) Ton-That, C. *Macromolecules* **2000**, *33*, 8453.
(50) Brochard Wyart, F.; Martin, P.; Redon, C. *Langmuir* **1993**, *9*, 3682. Brochard-Wyart, *Can. J. Phys.* **1990**, *68*, 1084.
(51) Rysz, J.; et al. *Europhys. Lett.* **2000**, *50*, 35.
(52) Geoghegan, M.; Ermer, H.; Jüngst, G.; Krausch, G.; Brenn, R. *Phys. Rev. E* **2000**, *62*, 940.
(53) Björström, C. M.; Nilsson, S.; Bernasik, A.; Budkowski, A.; Andersson, M.; Magnusson, K. O.; Moons, E. *Appl. Surf. Sci.* **2007**, *253*, 3906.

MA070712A